Available online at www.sciencedirect.com

Journal of Solid State Chemistry 179 (2006) 3636–3644

www.elsevier.com/locate/jssc

The intergrowth structure of $Ag_{1.2}Bi_{17.6}S_{23}Cl_8$ and its relation to the tubular structure of $Bi_{6+\delta}S_{6+3\delta}Cl_{6-3\delta}$ and the pavonite homologue $Ag_{3x}Bi_{5-3x}S_{8-6x}Cl_{6x-1}$

Pierre F.P. Poudeu[a,b], Michael Ruck[a,*]

[a]*Institute of Inorganic Chemistry, Dresden University of Technology, D-01062 Dresden, Germany*
[b]*Department of Chemistry, Michigan State University, East Lansing, MI 48824, USA*

Received 12 June 2006; received in revised form 19 July 2006; accepted 24 July 2006
Available online 27 July 2006

Abstract

The crystal structures of two members of the solid solution series $Bi_{6+\delta}S_{6+3\delta}Cl_{6-3\delta}$ and of $Ag_{1.2}Bi_{17.6}S_{23}Cl_8$ have been determined by single-crystal X-ray diffraction at room temperature. Single-crystals used for the investigations were obtained from a reaction involving Bi_2S_3 and AgCl in the molar ratio 3:2 at 740 K. $Bi_{6+\delta}S_{6+3\delta}Cl_{6-3\delta}$ compounds crystallize in the hexagonal space group $P6_3/m$ (no. 176) with $a = 11.427(2)$ Å, $c = 4.071(1)$ Å, for $\delta = 0.64$, and $a = 11.540(2)$ Å, $c = 4.040(1)$ Å, for $\delta = 0.86$ ($Z = 1$). The disordered structure of $Bi_{6+\delta}S_{6+3\delta}Cl_{6-3\delta}$ is closely related to the ordered rhombohedral structure of $Bi_4S_5Cl_2$. It consists of parallel six-membered ring channels of face- and edge-sharing bicapped trigonal prisms around Bi atoms with additional Bi atoms on the central axes. $Ag_{1.2}Bi_{17.6}S_{23}Cl_8$ adopts the monoclinic space group $C2/m$ (no. 12) with $a = 53.036(9)$ Å, $b = 4.030(1)$ Å, $c = 11.643(4)$ Å, $\beta = 94.4(1)°$, $Z = 2$. $Ag_{1.2}Bi_{17.6}S_{23}Cl_8$ adopts a new structure type that can be interpreted as a periodic layered intergrowth of modules from $Bi_{6+\delta}S_{6+3\delta}Cl_{6-3\delta}$ and the pavonite homologue $Ag_{3x}Bi_{5-3x}S_{8-6x}Cl_{6x-1}$ ($^{(2,\ x)}$P) along [1 0 0]. The detailed geometrical analysis reveals a remarkable similarity of the interface in the three structures.

Keywords: Silver; Bismuth; Chalcogenides; Halides; Intergrowth structures

---

1. Introduction

Synthetic investigations of ternary bismuth thiohalogenides have revealed the existence of several classes of compounds with various structure types. Besides the well-known ternary isostructural phases Bi*SX* ($X =$ Cl, Br, I) [1–6] and $Bi(Bi_2S_3)_9X_3$ ($X =$ Br, I), [7,8] the structure of $Bi_4S_5Cl_2$ [9] has also been described. The two latter classes of compounds belong to the zinckenite homologous series with general formula $M_{6+\delta+N(N+5)}A_{12+N(N+7)}$ ($\delta \leqslant 1$) where $M =$ cations and $A =$ anions, primarily sulfur atoms [10,11]. Their structures consist of six-membered ring channels of face- and edge-sharing bicapped trigonal prisms around bismuth atoms with additional bismuth atoms on the central axes. Adjacent sets of ring channels are separated by layers (with varying thickness) of edge-sharing monocapped trigonal prisms around Bi atoms. δ corresponds to the amount of Bi atoms found within the hexagonal channel and N is the number of polyhedra within the layers that separate adjacent hexagonal tubes.

Recently, our exploratory synthetic investigations of quaternary compounds in the systems Ag–Bi–Q–X ($Q =$ S, Se; $X =$ Cl, Br) have contributed to the discovery of a variety of phases with staggering compositional complexity and structural diversity. Among these are $Ag_2Bi_2S_3Cl_2$ [12], $AgBi_2Q_3Cl$ ($Q =$ S, Se) [13] and numerous members of the broad homologous series $[BiQX]_2 \cdot [Ag_xBi_{1-x}Q_{2-2x}X_{2x-1}]_{N+1} = Ag_{x(N+1)}Bi_{2+(1-x)(N+1)}Q_{2+(2-2x)(N+1)}X_{2+(2x-1)(N+1)}$ ($N \geqslant 0$; $1/2 \leqslant x \leqslant 1$; $C2/m$; $Z = 2$) [14–16] which are structurally characterized by two alternating types of modules denoted A and B. The A module, which is similar for all known members of the series, consists of paired monocapped trigonal prisms around Bi atoms, which

---

[*] Corresponding author. Fax: +49 351 463 37287.
E-mail address: Michael.Ruck@tu-dresden.de (M. Ruck).

0022-4596/$ - see front matter © 2006 Elsevier Inc. All rights reserved.
doi:10.1016/j.jssc.2006.07.034

alternate with octahedrally coordinated metal atoms (mixed occupied by Ag and Bi). The *B* module represents NaCl-like modules with varying thickness defined by *N*. Various members of this series can be denoted by $^{(N,\ x)}$P according to the nomenclature of pavonite homologues ^{N}P [17]. The discovery of $Ag_{1.2}Bi_{17.6}S_{23}Cl_8$, which does not belong to any of these classes of compounds, reveals another dimension of the rich chemistry of these systems. Here we present the crystal structures of $Bi_{6.64}S_{7.92}Cl_{4.08}$ and $Bi_{6.88}S_{8.64}Cl_{3.36}$, which are the members of the solid solution series $Bi_{6+\delta}S_{6+3\delta}Cl_{6-3\delta}$ with $\delta = 0.64$ and 0.88, as well as the crystal structure of the intergrowth compound $Ag_{1.2}Bi_{17.6}S_{23}Cl_8$ and its relation to the structures of $Bi_{6+\delta}S_{6+3\delta}Cl_{6-3\delta}$ and of the pavonite homologous series $[BiSCl]_2 \cdot [Ag_xBi_{1-x}S_{2-2x}Cl_{2x-1}]_3$ ($N = 2$).

2. Experimental section

2.1. Synthesis

Single crystals of $Bi_{6+\delta}S_{6+3\delta}Cl_{6-3\delta}$ with $\delta = 0.64$ **(I)** and 0.88 **(II)**, as well as of $Ag_{1.2}Bi_{17.6}S_{23}Cl_8$ were obtained as by-products during our investigation of quaternary compounds in the system Ag–Bi–S–Cl. A mixture of the starting materials Bi_2S_3 (Alfa Aesar, 99.9%) and AgCl (Merck, >99.4%) in the molar ratio 3:2 was ground and sealed in an evacuated silica tube. The tube was placed in a furnace and heated up to 740 K in 4 h. This temperature was maintained for 3 days, at which time the furnace was cooled down to room temperature at a rate of 5 K/min. The resulting black polycrystalline product contained single crystals, which could easily be separated into the studied phases on account of their habits (crystals of $Bi_{6+\delta}S_{6+3\delta}Cl_{6-3\delta}$ are black thin plates whereas those of $Ag_{1.2}Bi_{17.6}S_{23}Cl_8$ are black with needle-like shape). It was found that these phases coexist with $Ag_{3x}Bi_{5-3x}S_{8-6x}Cl_{6x-1}$ ($1/2 \leqslant x \leqslant 1$; $^{(2,\ x)}$P) [16].

2.2. EDX analysis

The EDX analysis was performed on the single crystal used for structure determinations. The investigation was aimed to check about the possible presence of Ag atoms in the crystal of **(I)** and **(II)** and also to determine the Ag to Bi ratio in $Ag_{1.2}Bi_{17.6}S_{23}Cl_8$. The experiment was performed on a digital scanning electron microscope LEO 982 (LEO Elektronenmikroskopie GmbH, Oberkochen, Germany). Data were acquired using an accelerating voltage of 15 kV and a 100 s accumulation time. The semi-quantitative analysis of the spectrum was performed with the program Analyse Voyager [18]. The result obtained shows no appreciable trace of Ag atoms in the crystal of **(I)** and **(II)**. The average compositions were $Ag_{0.1(2)}Bi_{6.6(2)}S_9Cl_3$ (for **(I)** and **(II)**) and $Ag_{1.0(2)}Bi_{17.5(2)}S_{25}Cl_6$.

2.3. Crystal structure determination

$Bi_{6+\delta}S_{6+3\delta}Cl_{6-3\delta}$. The zero and first level single crystal precession photographs of **(I)** and **(II)** recorded using a zirconium filtered molybdenum radiation on a Huber camera with imaging plate technique showed the Laue symmetry $6/m$ and reflection conditions ($0\,0\,l$ with $l = 2n$) suggesting $P6_3$ (no. 173) or $P6_3/m$ (no. 176) as possible space groups. No additional diffuse reflections that would identify a superstructure were observed. The same single crystals were used for the collection of intensity data. Details on the measuring parameters are given in Table 1. The structure was solved with direct methods [19] in the space group $P6_3/m$. The refinement of the 31 parameters was performed by the full matrix least square techniques [19]. The solution revealed all atom positions in the asymmetric unit. In the first step of the refinement, the two Bi atoms Bi(1) and Bi(2) displayed extraordinary large temperature factors and the agreement factor R_1 was very poor (about 30%). The two atoms were split into pairs of statistically occupied close positions Bi(1a), Bi(1b) and Bi(2a), Bi(2b). After preliminary free refinement of their occupancies the atoms in Bi(2a)/Bi(2b) split positions were constrained to display the same thermal parameter with equal occupancy factor. The total occupancies refined to 100% for Bi(1a/1b), and 64(1)% or 88(1)% for Bi(2a/2b) in **(I)** and **(II)**. A mixed occupation with Ag and Bi at the Bi(2) position was also considered. However, EDX as well as crystal chemical considerations, discussed in detail below, clearly point to a partial occupancy of the Bi(2a/2b) positions by Bi rather than an Ag/Bi mixed occupation. The compositions of the crystals, $Bi_{6.64(1)}S_{7.92(3)}Cl_{4.08(3)}$ **(I)** and $Bi_{6.88(1)}S_{8.64(3)}Cl_{3.36(3)}$ **(II)**, were assigned based on the results of the refinement of the Bi positions and by considering the electroneutrality requirements. It was necessary to assume a S/Cl mixed occupation in both anions positions $Z(1)$ and $Z(2)$. Fractional atomic coordinates and isotropic displacement parameters are gathered in Table 2. The parameters for the two studied crystals are grouped according to the Wyckoff position and with respect to the increase in δ. A synopsis of selected interatomic distances is given in Table 3.

$Ag_{1.2}Bi_{17.6}S_{23}Cl_8$. Precession photographs of the single crystal of $Ag_{1.2}Bi_{17.6}S_{23}Cl_8$ showed the monoclinic Laue class $2/m$ with the reflection conditions $h+k = 2n$ for all $h\,k\,l$ indicating $C2$ (no. 5), Cm (no. 8) or $C2/m$ (no. 12) as possible space groups. A rotation photograph of the same crystal mounted parallel to [0 1 0] showed no trace of diffuse streaks or superstructure reflections. The same single crystal was used for the collection of intensity data. Details on the measuring parameters are given in Table 1. Assuming the space group $C2/m$, the structure solution revealed the positions of all bismuth and silver atoms together with some of the anion positions. In subsequent refinement steps the positions of the remaining anions were deduced from difference Fourier syntheses. Nine bismuth atoms Bi(1–9) and one silver atom Ag(1) were found in the

Table 1
Selected crystallographic data and details of the structure determinations of $Bi_{6+\delta}S_{6+3\delta}Cl_{6-3\delta}$ ($\delta = 0.64$ (**I**) and 0.88 (**II**)) and of $Ag_{1.2}Bi_{17.6}S_{23}Cl_8$

Formula	$Bi_{6.64(1)}S_{7.92(3)}Cl_{4.08(3)}$ (**I**)	$Bi_{6.88(1)}S_{8.64(3)}Cl_{3.36(3)}$ (**II**)	$Ag_{1.2(1)}Bi_{17.6(1)}S_{23}Cl_8$
Formula weight (g/mol)	1786.2	1829.3	4829.6
Crystal system	Hexagonal	Hexagonal	Monoclinic
Space group	$P6_3/m$ (no. 176)	$P6_3/m$ (no. 176)	$C2/m$ (no. 12)
Crystal size (mm^3); colour	$0.05 \times 0.02 \times 0.01$; black	$0.05 \times 0.03 \times 0.03$; black	$0.07 \times 0.04 \times 0.03$; black
Density (ρ_{cal}) (g/cm^3)	6.44	6.52	6.46
Lattice parameters	Refined from the total collected single crystal reflections		
(Å; °)	$a = 11.427(2)$	11.540(2)	53.036(9)
	$b = a$	a	4.030(1)
	$c = 4.071(1)$	4.040(1)	11.643(4)
	$\beta = 90°$	90°	94.4(1)
V (Å^3); Z	460.4(2); 1	465.9(2); 1	2481.2(2); 2
Radiation (Å)	$\lambda(MoK_\alpha) = 0.71073$	$\lambda(MoK_\alpha) = 0.71073$	$\lambda(AgK_\alpha) = 0.56087$
Temperature (K)	298(1)	298(1)	293(1)
2θ range; index range	$7° \leqslant 2\theta \leqslant 56°$; $-15 \leqslant h, k \leqslant 15$, $-5 \leqslant l \leqslant 5$	$8° \leqslant 2\theta \leqslant 56°$; $-15 \leqslant h, k \leqslant 15$, $-4 \leqslant l \leqslant 4$	$2.8° \leqslant 2\theta \leqslant 38.9°$; $-60 \leqslant h \leqslant 62$, $-4 \leqslant k \leqslant 4$, $-13 \leqslant l \leqslant 13$
Measured reflections	4188	3921	7412
Unique reflections	407	396	2500
Reflec. With $F_o > 4\sigma(F_o)$	314	350	1586
R_{int}/R_σ	0.097/0.041	0.067/0.023	0.072/0.094
Absorption correction	Numerical, crystal description optimized using equivalent reflections		
μ (cm^{-1})	647	660	350
Transmission factors	0.34–0.51	0.14–0.27	0.19–0.47
Structure refinement	Least-squares method; full matrix; based on F^2; anisotropic displacement parameters [18]		
Residual electron density (e Å^{-3})	+1.62 to −1.92	+1.12 to −1.31	+7.00 to −5.80
$R_1(F_o > 4\sigma(F_o))^{(a)}$	0.046	0.041	0.044
$wR_2(all)^{(b)}$	0.095	0.103	0.053
GooF	1.057	1.097	0.992
m; n	0.028; 21.990	0.052; 6.826	0; 0

(a) $R_1 = \Sigma||F_o| - |F_c||/\Sigma|F_o|$;
(b) $wR_2 = \{\Sigma w(F_o^2 - F_c^2)2/\Sigma[w(F_o^2)^2]\}^{1/2}$, $w^{-1} = \sigma^2(F_o^2) + (mP)^2 + nP$, $P = (F_o^2 + 2F_c^2)/3$.

Table 2
Wyckoff positions, occupancies (k), coordinates, and equivalent isotropic displacement parameters U_{eq} (10^{-4} Å^2)[a] for the atoms in the asymmetric unit of $Bi_{6.64}S_{7.92}Cl_{4.08}$ ($\delta = 0.64$) and of $Bi_{6.88}S_{8.64}Cl_{3.36}$ ($\delta = 0.88$; below), Z = S/Cl

Atom	Wyck.	k	x	y	z	U_{eq}
Bi(1a)	6h	0.69(1)	0.2536(2)	0.4003(4)	1/4	242(6)
		0.67(1)	0.2521(1)	0.4031(1)	1/4	323(4)
Bi(1b)	6h	0.31(1)	0.2979(6)	0.4105(8)	1/4	300(3)
		0.33(1)	0.3130(3)	0.4213(2)	1/4	294(6)
Bi(2a)	4h	0.08(1)	0	0	0.29(2)	271(2)
		0.11(1)	0	0	0.30(5)	290(2)
Bi(2b)	4h	0.08(1)	0	0	0.075(2)	271(2)
		0.11(1)	0	0	0.07(1)	290(2)
Z(1)	6h	0.66(2)/0.34(2)	−0.0099(5)	0.2236(5)	1/4	180(2)
		0.72(2)/0.28(2)	−0.0090(3)	0.2305(3)	1/4	245(7)
Z(2)	6h	0.66(2)/0.34(2)	0.5163(5)	0.3790(5)	1/4	200(2)
		0.72(2)/0.28(2)	0.5173(3)	0.3790(3)	1/4	235(7)

Standard deviations corresponding to the last digit are indicated in brackets.
[a] U_{eq} is defined as one-third of the trace of the orthogonalized U_{ij} tensor.

asymmetric unit. The displacement parameter of Bi(2) was high compared to those of the other bismuth atoms, we assumed that the bismuth on the M(2) position is partially substituted by silver. This idea was supported by crystal chemical analogies from the $[BiSCl]_2 \cdot [Ag_xBi_{1-x}S_{2-2x}Cl_{2x-1}]_{N+1}$ homologous series. On the other hand, high residual electron density was observed around Bi(8) and Bi(9). These atoms were then split into two pairs of close positions. The total occupancies refined to 100% for Bi(8a/8b), and 91(1)% for Bi(9a/9b). The differentiation between

Table 3
Selected interatomic distances (Å) for $Bi_{6.64}S_{7.92}Cl_{4.08}$ ($\delta = 0.64$) and $Bi_{6.88}S_{8.64}Cl_{3.36}$ ($\delta = 0.88$), Z = S/Cl

	$\delta = 0.64$	$\delta = 0.88$
Bi(1a)		
$Z(1)$	2.658(5)	2.654(3)
$Z(1^{i}, 1^{ii})$	2.691(3)	2.690(1)
$Z(2^{iii}, 2^{iv})$	3.071(5)	3.045(3)
$Z(2)$	3.131(7)	3.208(4)
$Z(2^{v}, 2^{vi})$	3.284(4)	3.285(2)
Bi(1b)		
$Z(2)$	2.693(2)	2.636(5)
$Z(1^{i}, 1^{ii})$	2.690(5)	2.719(1)
$Z(2^{v}, 2^{vi})$	3.055(5)	2.952(2)
$Z(1)$	3.069(7)	3.236(3)
$Z(2^{iii}, 2^{iv})$	3.346(8)	3.407(3)
Bi(2a)		
$Z(1, 1^{xiv}, 1^{xv})$	2.619(3)	2.721(2)
$Z(1^{ii}, 1^{iii}, 1^{xii})$	3.215(3)	3.266(2)
$Z(1^{i}, 1^{iv}, 1^{x})$	3.415(4)	3.507(2)
Bi(2b)		
$Z(1, 1^{xiv}, 1^{xv})$	2.709(2)	2.810(2)
$Z(1^{i}, 1^{iv}, 1^{x})$	2.929(3)	3.004(3)

Standard deviations corresponding to the last digit are indicated in brackets.

Operators for generating equivalent atoms: (i) $y, -x+y, -z$; (ii) $y, -x+y, 1-z$; (iii) $x-y, x, 1-z$; (iv) $x-y, x, -z$; (v) $1-x, 1-y, 1-z$; (vi) $1-x, 1-y, -z$; (vii) $x, y, 1+z$; (viii) $x, y, -1+z$; (ix) $x, y, 1/2-z$; (x) $-x, -y, -z$; (xi) $-x, -y, 1/2+z$; (xii) $-x, -y, 1-z$; (xiii) $-x, -y, -1/2+z$; (xiv) $-y, x-y, z$; (xv) $-x+y, -x, z$.

Table 4
Wyckoff positions, occupancies (k), coordinates, and equivalent isotropic displacement parameters U_{eq} (10^{-4} Å^2)[a] for the atoms in the asymmetric unit of $Ag_{1.2}Bi_{17.6}S_{23}Cl_8$

Atom	Wyck.	k	x	y	z	U_{eq}
Bi(1)	4i	1	0.04324(2)	$\frac{1}{2}$	0.78245(9)	237(3)
M(2)	4i	[b]	0.02804(2)	0	0.39412(9)	247(5)
Bi(3)	4i	1	0.10985(2)	$\frac{1}{2}$	0.4952(1)	342(3)
Bi(4)	4i	1	0.07293(2)	0	0.08152(9)	221(3)
Bi(5)	4i	1	0.12619(2)	$\frac{1}{2}$	−0.10929(9)	237(3)
Bi(6)	4i	1	0.21403(2)	0	−0.02642(9)	313(3)
Bi(7)	4i	1	0.23098(2)	$\frac{1}{2}$	0.2994(1)	291(3)
Bi(8a)	4i	0.5	0.17636(6)	0	0.5990(3)	202(7)
Bi(8b)	4i	0.5	0.18486(6)	0	0.5636(3)	218(7)
Bi(9a)	4i	0.458(4)	0.15328(6)	0	0.2169(3)	395(9)
Bi(9b)	8j	0.226(4)	0.15349(8)	0.199(2)	0.2136(3)	390(2)
Ag(1)	2a	1	0	0	0	302(9)
S(1)	4i	1	−0.0084(1)	0	0.2163(5)	120(2)
S(2)	2d	1	0	$\frac{1}{2}$	1/2	380(4)
S(3)	4i	1	0.0379(1)	$\frac{1}{2}$	0.0027(5)	100(2)
S(4)	4i	1	0.0822(1)	0	0.8660(5)	130(2)
S(5)	4i	1	0.1098(1)	$\frac{1}{2}$	0.0956(6)	200(3)
S(6)	4i	1	0.1090(1)	0	0.3374(5)	220(3)
S(7)	4i	1	0.1304(1)	0	0.6635(5)	130(2)
S(8)	4i	1	0.1548(1)	0	−0.0198(6)	210(3)
S(9)	4i	1	0.1580(1)	$\frac{1}{2}$	0.4573(5)	150(2)
S(10)	4i	1	0.1988(1)	$\frac{1}{2}$	0.1116(5)	130(2)
S(11)	4i	1	0.2005(1)	0	0.3501(5)	140(3)
S(12)	4i	1	0.2528(1)	0	0.1304(5)	170(3)
Cl(1)	4i	1	0.0540(1)	$\frac{1}{2}$	0.2927(6)	270(3)
Cl(2)	4i	1	0.0649(1)	0	0.5806(5)	230(3)
Cl(3)	4i	1	0.1827(1)	$\frac{1}{2}$	0.7788(5)	190(3)
Cl(4)	4i	1	0.2275(1)	$\frac{1}{2}$	0.5734(5)	230(3)

Standard deviations corresponding to the last digit are indicated in brackets.

[a] U_{eq} is defined as one-third of the trace of the orthogonalized U_{ij} tensor.

[b] $M(2) = 0.888(4)\text{Bi} + 0.112(4)\text{Ag}$.

the S and Cl positions was evaluated by calculating the bond valence sums [20]. From the final refinement, after absorption correction and including the secondary extinction correction as well as anisotropic displacement parameters for all atoms, the composition of the crystal was defined as $Ag_{1.2(1)}Bi_{17.6(1)}S_{23}Cl_8$. The coordinates and isotropic displacement parameters of all atoms are given in Table 4. Selected interatomic distances are gathered in Table 5. Further details of the crystal structure investigations can be obtained from the Fachinformationszentrum Karlsruhe, 76344 Eggenstein-Leopoldshafen, Germany, (fax: +49 7247 808 666; e-mail: crysdata@fiz.karlsruhe.de) on quoting the depository number CSD−416683 ($Bi_{6.88}S_{8.64}Cl_{3.36}$), CSD−416684 ($Bi_{6.64}S_{7.92}Cl_{4.08}$) and CSD−416685 ($Ag_{1.2}Bi_{17.6}S_{23}Cl_8$). The graphic representation of the crystal structures were created with the program Diamond [21] using the ellipsoid representation (95% probability level) for all atoms.

3. Results and discussion

3.1. Structure description and discussion

$Bi_{6+\delta}S_{6+3\delta}Cl_{6-3\delta}$. $Bi_{6.64}S_{7.92}Cl_{4.08}$ **(I)** ($\delta = 0.64$) and $Bi_{6.88}S_{8.64}Cl_{3.36}$ **(II)** ($\delta = 0.88$) are two members of the series of compounds with the general formula $Bi_{6+\delta}S_{6+3\delta}Cl_{6-3\delta}$ with $\delta \leqslant 1$. The structural motif associated to this class of compounds is represented in Fig. 1. In the structure, the bismuth atoms located on the 6_3 axes, i.e. Bi(2a/2b), are surrounded by a six-membered ring of edge-sharing bicapped trigonal prisms around Bi(1a/1b). The bicapped trigonal prisms further share their triangular faces along [0 0 1] to form hexagonal tubes. The tubes are linked via common edges and form a special type of hexagonal rod packing with empty trigonal channels.

The bismuth atoms inside the hexagonal tubes adopt two different types of coordination. The Bi(2a) displays a tricapped trigonal prismatic coordination (c.n. = 9) while Bi(2b) is located in a trigonally compressed, octahedral environment (Fig. 2a). These polyhedra are arranged in such a way that the octahedron shares all its coordination with the tricapped trigonal prisms. This arrangement, in addition to the $6/m$ symmetry of the structure causes the split positions to align in very close positions about 0.93 Å apart (Fig. 2b). In total there are 0.64 in **(I)** or 0.88 bismuth atoms per unit cell in **(II)** distributed over eight split positions. This results in average Bi–Bi distances of 6.36 and 4.59 Å.

Table 5
Selected interatomic distances (Å) in $Ag_{1.2}Bi_{17.6}S_{23}Cl_8$

Bi(1)		Bi(7)	
$S(3^{x})$	2.602(6)	$S(10)$	2.668(7)
$S(1^{vi}, 1^{vii})$	2.736(5)	$S(11, 11^{v})$	2.676(4)
$S(4, 4^{v})$	2.996(5)	$S(12, 12^{v})$	3.102(5)
$Cl(2, 2^{v})$	3.365(5)	$Cl(4)$	3.210(7)
$S(2)$	3.862(2)	$Cl(4^{xiv}, 4^{xv})$	3.257(6)
Bi(2)		Bi(8a)	
$S(1)$	2.720(7)	$S(7)$	2.607(7)
$Cl(1, 1^{iv})$	2.756(4)	$S(9, 9^{iv})$	2.735(6)
$Cl(2)$	2.809(7)	$Cl(3, 3^{iv})$	2.907(6)
$S(2, 2^{iv})$	2.841(1)	$S(11)$	3.257(7)
		$Cl(4, 4^{iv})$	3.409(6)
Bi(3)		Bi(8b)	
$S(9)$	2.594(7)	$S(11)$	2.681(7)
$S(6, 6^{v})$	2.725(5)	$S(9, 9^{iv})$	2.710(6)
$S(7, 7^{v})$	2.959(5)	$Cl(4, 4^{iv})$	3.023(6)
$Cl(2, 2^{v})$	3.329(5)	$S(7)$	3.197(7)
$Cl(1)$	3.643(8)	$Cl(3, 3^{iv})$	3.225(6)
Bi(4)		Bi(9a)	
$S(4^{ii})$	2.594(6)	$S(8)$	2.763(8)
$S(5, 5^{iv})$	2.804(5)	$S(6)$	2.828(8)
$S(3, 3^{iv})$	2.846(5)	$S(11)$	2.844(8)
$Cl(1, 1^{iv})$	3.391(5)	$S(5, 5^{iv})$	3.297(7)
$S(6)$	3.414(7)	$S(9, 9^{iv})$	3.442(6)
		$S(10, 10^{iv})$	3.442(6)
Bi(5)		Bi(9b)	
$S(5)$	2.601(7)	$S(8)$	2.839(8)
$S(8, 8^{v})$	2.685(5)	$S(5)$	2.871(9)
$S(4^{ii}, 4^{iii})$	3.078(5)	$S(11)$	2.964(8)
$S(7^{ii}, 7^{iii})$	3.347(5)	$S(6)$	2.969(8)
$Cl(3^{ii})$	3.357(6)	$S(10)$	3.016(8)
		$S(9)$	3.079(8)
Bi(6)		Ag(1)	
$S(12)$	2.644(7)	$S(1, 1^{viii})$	2.590(6)
$S(10, 10^{iv})$	2.738(4)	$S(3, 3^{iv}, 3^{viii}, 3^{xx})$	2.844(4)
$S(12^{xii}, 12^{xiii})$	2.992(5)		
$S(8)$	3.147(7)		
$Cl(3^{i}, 3^{ii})$	3.374(6)		

Standard deviations corresponding to the last digit are indicated in brackets.

Operators for generating equivalent atoms: (i) $x, y-1, z-1$; (ii) $x, y, z-1$; (iii) $x, y+1, z-1$; (iv) $x, y-1, z$; (v) $x, y+1, z$; (vi) $-x, -y, 1-z$; (vii) $-x, -y+1, 1-z$; (viii) $-x, -y, -z$; (ix) $x, y-1, z+1$; (x) $x, y, z+1$; (xi) $x, y+1, z+1$; (xii) $1/2-x, -y-1/2, -z$; (xiii) $1/2-x, 1/2-y, -z$; (xiv) $1/2-x, 1/2-y, 1-z$; (xv) $1/2-x, 1/2-y, 1-z$; (xvi) $x, -1-y, z$; (xvii) $x, -y, z$; (xviii) $x, 1-y+1, z$; (xix) $-x, -1-y, -z$; (xx) $-x, 1-y, -z$.

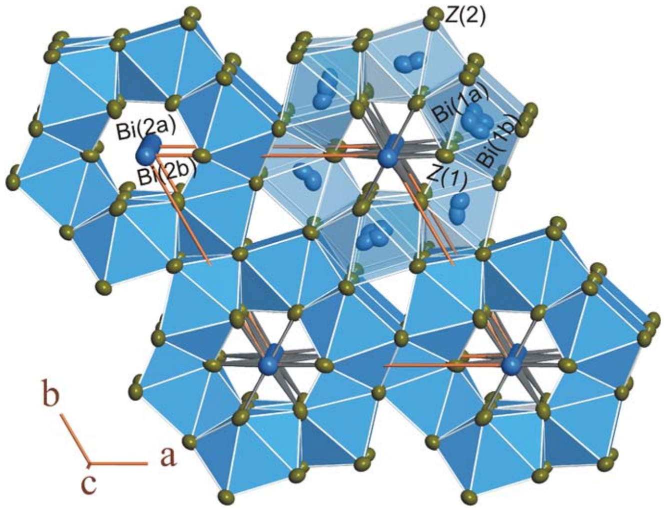

Fig. 1. The hexagonal structure of $Bi_{6+\delta}S_{6+3\delta}Cl_{6-3\delta}$ ($\delta \leqslant 1$) with atom labeling projected along [0 0 1].

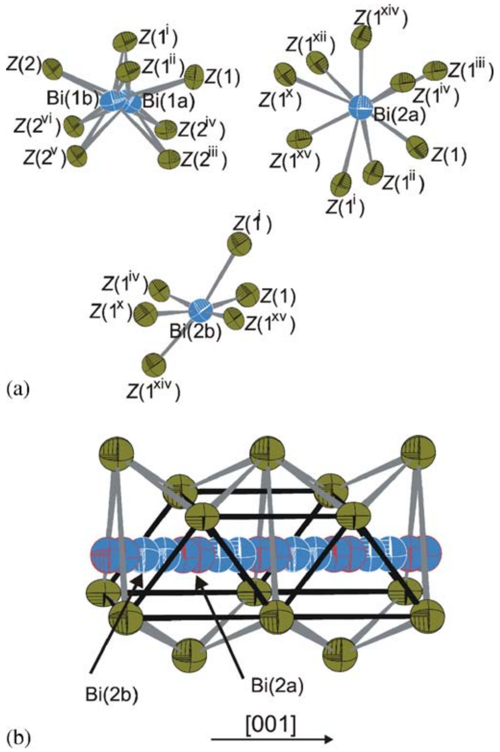

Fig. 2. (a) Environment of cations in $Bi_{6+\delta}S_{6+3\delta}Cl_{6-3\delta}$. Ellipsoids correspond to 95% probability level. For bond distances see Table 3, (b) Positional disorder of Bi(2) atoms inside the channel form by the network of face-sharing trigonal prisms.

The channel structure of $Bi_{6+\delta}S_{6+3\delta}Cl_{6-3\delta}$ is closely related to the rhombohedral structure of the sulfide chloride "$Bi_4S_5Cl_2$"[1] [9]. The principal arrangement of atoms is the same in both structures except for the distribution of the bismuth atoms inside the channel. In the rhombohedral structure ($a_{rh} \approx \sqrt{3}a_{hex}$, $c_{rh} \approx 3c_{hex}$, $V_{rh} \approx 9V_{hex}$), the atoms are ordered within the hexagonal channels while in the hexagonal structure, a positional disorder is observed. The variable amount of bismuth that can be found inside the channel is connected with the substitution in anion positions of univalent chlorine atoms by bivalent sulfur atoms. This substitution yields a series of isostructural compounds with general formula $Bi_{6+\delta}S_{6+3\delta}Cl_{6-3\delta}$, where δ corresponds to the amount of

---

[1] The compound was assigned the formula $Bi_4S_5C_{12}$. With $Z = 15$ the content of the rhombohedral unit cell would be represented by $Bi_{60}S_{75}Cl_{30}$ ($Z = 1$). On the contrary the original crystal structure determination comprises 108 anions per unit cell and nothing is reported about any anion deficiency. Therefore we assume the correct formula should be $Bi_{60}S_{72}Cl_{36}$ ($Z = 1$) or $Bi_5S_6Cl_3$ ($Z = 12$) or, for our purpose, $Bi_{6.67}S_8Cl_4$ ($Z = 9$).

bismuth found inside the channel. With regard to the translational period in [0 0 1] we assume an upper limit of $\delta \leqslant 1$. The composition obtained from the structure refinement of **(I)**, $\delta = 0.64$, is close to that of the ordered variant $Bi_{6.67}S_8Cl_4$ ($\delta = 2/3$) [9] but the superstructure reported for "$Bi_4S_5Cl_2$" is not observed. This may result from different synthesis routes, which were crystallization from the melt in the case of **(I)** and **(II)** but vapor deposition in the case of "$Bi_4S_5Cl_2$".

According to the lattice parameters of $Bi_{6.64}S_{7.92}Cl_{4.08}$ **(I)** and $Bi_{6.88}S_{8.64}Cl_{3.36}$ **(II)** (Table 1) an increase of the bismuth content inside the channel causes an anisotropic expansion of the framework ($\Delta V/V = 1.2\%$). The variability of the cell parameters with increasing δ is positive in [1 0 0] ($\Delta a/a = 1\%$) and negative in [0 0 1] ($\Delta c/c = -0.8\%$). The interatomic distances around Bi(2) are also affected (Table 3).

(I) and **(II)** can also be viewed as non-stoichiometric members of the zinckenite homologous series $M_{6+\delta+N(N+5)}A_{12+N(N+7)}$ where N is the number of polyhedra within the layers that separate adjacent hexagonal tubes. The hexagonal structure of $Bi_{6+\delta}S_{6+3\delta}Cl_{6-3\delta}$ corresponds to the case $N = 0$. Other known members of the series include $Pb_7S_2Br_{10}$ ($N = 0$, $\delta = 1$) [21], Th_7S_{12} ($N = 0$, $\delta = 1$) [22], $Bi(Bi_2S_3)_9X_3$ ($N = 1$, $\delta = 2/3$; X = Br, I) [7,8] and zinckenite $Pb_9Sb_{22}S_{42}$ ($N = 3$, $\delta = 1$) [10,11]. The existence of the hexagonal substructure of "$Bi_4S_5Cl_2$" has been predicted in order to satisfy the cell requirements necessary for the member $N = 0$ of the zinckenite homologous series [11].

In the view of the general characteristic of various members of the zinckenite homologous series (such as the incomplete occupation of the hexagonal channel) and the existence of triangular "empty" channels between three neighboring hexagonal tubes, the series $Bi_{6+\delta}S_{6+3\delta}Cl_{6-3\delta}$ offers possibilities of designing numerous isostructural compounds. In fact the variation of charge generated by the substitution of sulfur by chlorine can be compensated either by varying the bismuth content inside the channels or by addition of small size cations such as copper that may reside in the empty triangular channel or undergo mixed site occupation with the bismuth atoms inside the hexagonal channel. In the first case the variation of the S/Cl ratio may hypothetically generate isostructural compounds with composition ranging between BiSCl ($\delta = 0$) and $Bi_7S_9Cl_3$ ($\delta = 1$). For the bismuth-poor end member ($\delta = 0$) the hexagonal structure of the series collapses in favor of the orthorhombic structure adopted by BiSCl. That structure shows the same type of coordination polyhedra as $Bi_{6+\delta}S_{6+3\delta}Cl_{6-3\delta}$ but only one type of channel which is defined by a four-membered ring of edge-sharing bicapped trigonal prisms. In the case of the bismuth-rich end member ($\delta = 1$), the hexagonal structure may be maintained as can be seen for the structures of $Pb_7S_2Br_{10}$ [22] and Th_7S_{12} [23].

$Ag_{1.2}Bi_{17.6}S_{23}Cl_8$. $Ag_{1.2}Bi_{17.6}S_{23}Cl_8$ crystallizes with two formula units in the monoclinic space group $C2/m$ and adopts a new structure type. A polyhedra representation of the structure projected along [0 1 0] is shown in Fig. 3. As depicted in the figure, the structure of $Ag_{1.2}Bi_{17.6}S_{23}Cl_8$ can be subdivided into two distinct types of complex building units, denoted by "$Bi_{6+\delta}S_{6+3\delta}Cl_{6-3\delta}$" and "$^{(2,\ x)}P$", that alternate along [1 0 0].

The module "$Bi_{6+\delta}S_{6+3\delta}Cl_{6-3\delta}$" contains one six-fold coordinated bismuth atom, Bi(9b), six eight-fold coordinated bismuth atoms, Bi(3)–Bi(8), and one nine-fold coordinated bismuth atom, Bi(9a). All bismuth atoms with coordination number (c.n.) = 8 exhibit a bicapped trigonal prismatic environment of S and Cl (Fig. 4) with various degree of distortion (the geometry of their coordination polyhedra are of the types [1+2+2+2+1] or [1+2+2+1+2]). These polyhedra differ from each other

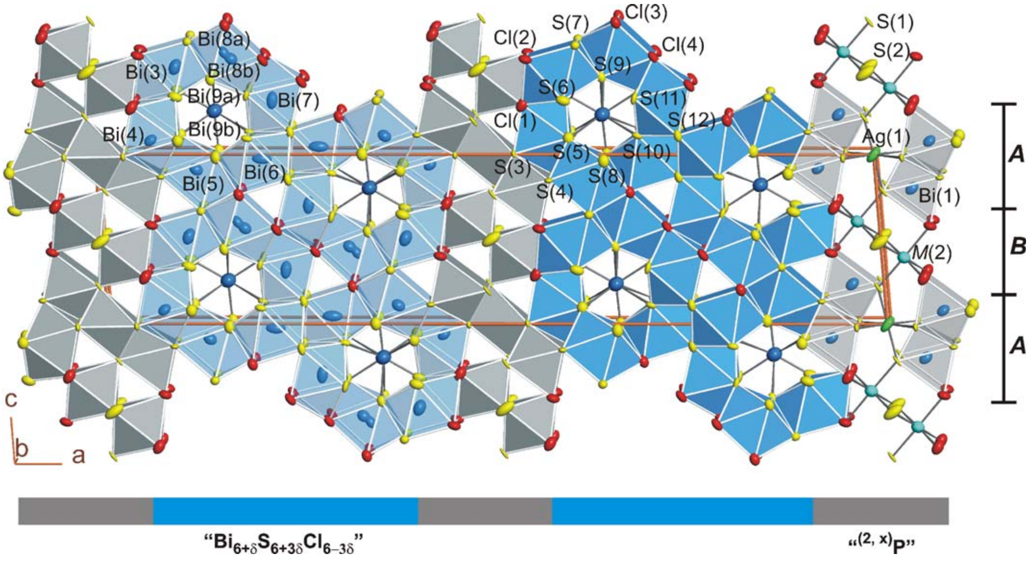

Fig. 3. A polyhedral representation of the structure of $Ag_{1.2}Bi_{17.6}S_{23}Cl_8$ with atom labeling projected along [0 1 0]. The two alternating types of structural units that build the structure are highlighted.

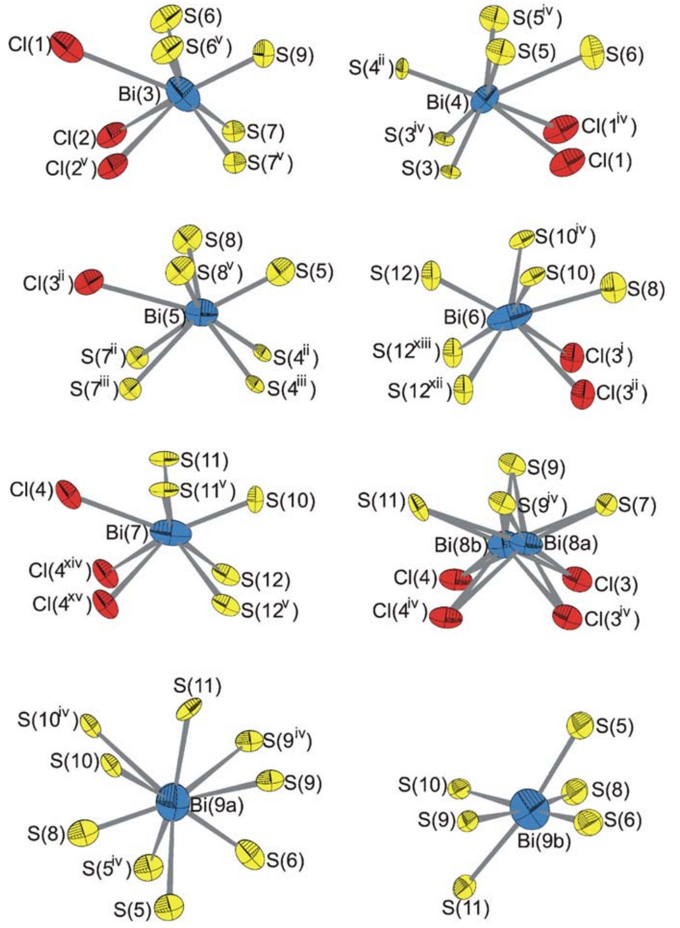

Fig. 4. Environment of cations in "Bi$_{6+\delta}$S$_{6+3\delta}$Cl$_{6-3\delta}$" structural unit of Ag$_{1.2}$Bi$_{17.6}$S$_{23}$Cl$_8$. Ellipsoids correspond to 95% probability level. For bond distances see Table 5.

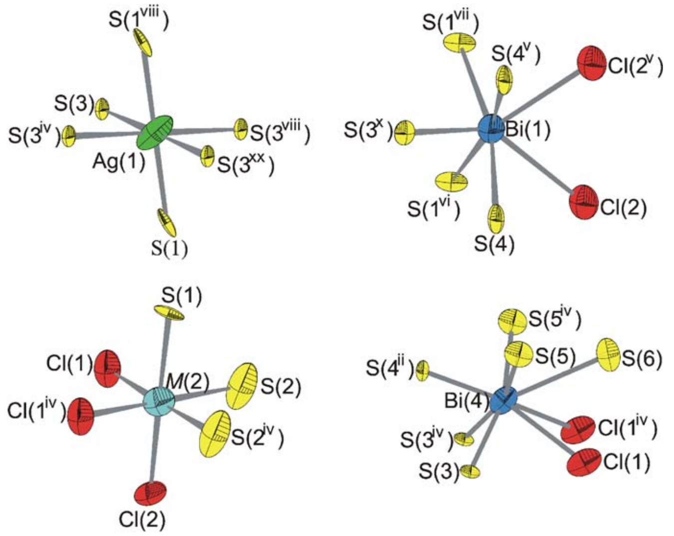

Fig. 5. Environment of cations in the "$^{(2,\ x)}$P" structural unit of Ag$_{1.2}$Bi$_{17.6}$S$_{23}$Cl$_8$. Ellipsoids correspond to 95% probability level. For bond distances see Table 5.

by the number and the arrangement of S and Cl in their coordination (Table 5). The composition of the polyhedra varies from [BiS$_7$Cl] to [BiS$_4$Cl$_4$]. The coordination polyhedra around Bi(9a) and Bi(9b) are, respectively, similar to those described above for Bi(2a) and Bi(2b) in the structure of Bi$_{6+\delta}$S$_{6+3\delta}$Cl$_{6-3\delta}$.

The arrangement of atoms in this structural unit is almost the same as the one described in the structure of Bi$_{6+\delta}$S$_{6+3\delta}$Cl$_{6-3\delta}$. The only structural difference is the amount of bismuth atoms inside the channel. In the present case there are 0.91 Bi per channel and translational period in [0 1 0] direction. This results in a mean Bi–Bi distance of 4.43 Å.

The large thermal parameter observed for Bi(9a) and Bi(9b) atoms (about 395×10^{-4} Å^2) is probably caused by the positional disorder inside the channel and indicates either possible "rattling" of these atoms about their crystallographic site or further splitting of positions.

The structural unit denoted "$^{(2,\ x)}$P" consists of polyhedra around the atoms Bi(1), *M*(2), Ag(1) and Bi(4). The Bi(1) atom is located in a monocapped trigonal prismatic coordination of five sulfur and two chlorine atoms. The additional *S*(2) atom that may complete the coordination to a bicapped trigonal prisms is situated at about 3.86 Å. The Bi(4) atom, which is common to the two types of building units, displays a bicapped trigonal prismatic coordination of six sulfur and two chlorine atoms. The geometry of the coordination polyhedron is similar to that of Bi(1) with one additional sulfur atom at 3.41 Å. The *M*(2) position exhibits a slightly distorted octahedral environment of three sulfur and three chlorine atoms. This coordination is distorted toward a trigonal bipyramid with short bonds *trans* to long bonds. The *M*(2) position in the structure shows mixed occupation between Ag and Bi with a large preference for the Bi atom (88.9%). The single Ag(1) atom is [2+4] coordinated by sulfur atoms with two short bonds in *trans* position and four long bonds in square plane (Fig. 5). The atomic arrangement in this building unit is essentially the same as in the structure of the pavonite homologous series Ag$_{3x}$Bi$_{5-3x}$S$_{8-6x}$Cl$_{6x-1}$ = [BiSCl]$_2\cdot$[Ag$_x$Bi$_{1-x}$S$_{2-2x}$Cl$_{2x-1}$]$_3$ ($1/2 \leqslant x \leqslant 1$; $^{(2,\ x)}$P) [16] (Fig. 6).

The complete structure of Ag$_{1.2}$Bi$_{17.6}$S$_{23}$Cl$_8$ is constructed by connecting side by side the two alternating types of structural units through the bicapped trigonal prisms around Bi(4) (Fig. 7). The structure of Ag$_{1.2}$Bi$_{17.6}$S$_{23}$Cl$_8$ can thus be interpreted as a layered intergrowth of the two structure types.

3.2. Structural relationships between Bi$_{6+\delta}$S$_{6+3\delta}$Cl$_{6-3\delta}$, Ag$_{3x}$Bi$_{5-3x}$S$_{8-6x}$Cl$_{6x-1}$ ($^{(2,\ x)}$P) and Ag$_{1.2}$Bi$_{17.6}$S$_{23}$Cl$_8$

The apparent structural relation of the intergrowth structure Ag$_{1.2}$Bi$_{17.6}$S$_{23}$Cl$_8$ with Bi$_{6+\delta}$S$_{6+3\delta}$Cl$_{6-3\delta}$, the hexagonal $N=0$ member of the zinckenite homologous series, and monoclinic Ag$_{1.59}$Bi$_{3.42}$S$_{4.83}$Cl$_{2.17}$, representing the homologue with $N=2$ and $x=0.53$ of the homologous series [BiSCl]$_2\cdot$[Ag$_x$Bi$_{1-x}$S$_{2-2x}$Cl$_{2x-1}$]$_{N+1}$ [16], can

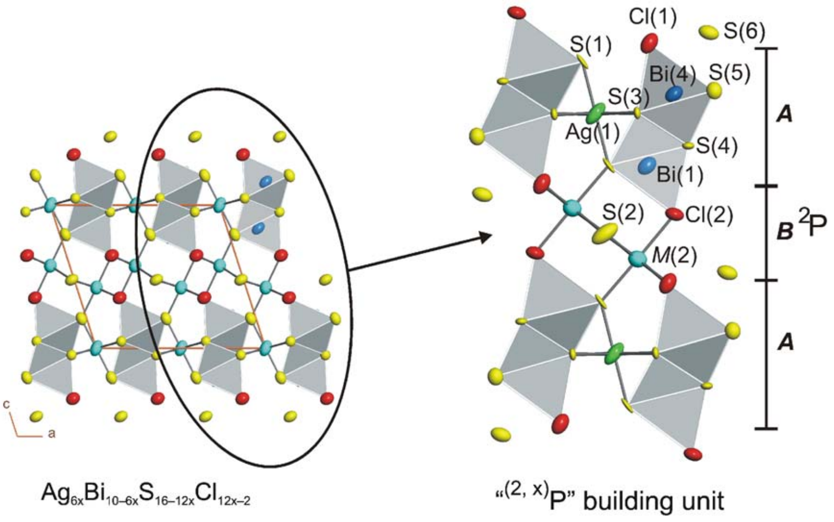

Fig. 6. The structure of $Ag_{3x}Bi_{5-3x}S_{8-6x}Cl_{6x-1}$ showing a possible cut of the "$^{(2,\,x)}$P" type building unit [16].

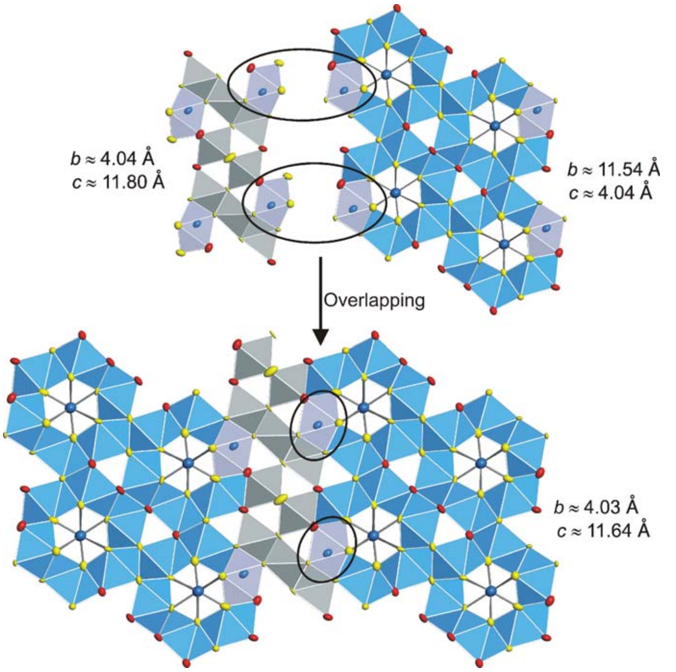

Fig. 7. Modular construction of the structure of $Ag_{1.2}Bi_{17.6}S_{23}Cl_8$. The two types of building units are connected through the bicapped trigonal prisms around Bi(4).

be quantified by analyzing the cation coordination in the three compounds using the polyhedron distortion parameters *v* (volume distortion), *Ecc*$_v$ (eccentricity) and *Sph*$_v$ (sphericity) recently devised by Mackovicky et al. [24,25]. Table 6 gives a synopsis of the calculated values for $Ag_{1.2}Bi_{17.6}S_{23}Cl_8$ and those of corresponding polyhedra in the structures of $Ag_{1.59}Bi_{3.42}S_{4.83}Cl_{2.17}$ ($^{(2,\,x)}$P;$x = 0.53$) and $Bi_{6.88}S_{8.64}Cl_{3.36}$ **(II)**.

The polyhedra around Bi(3)–Bi(8), which form the hexagonal tube in the intergrowth structure, show almost the same value of the three distortion parameters. This result is in agreement with our description according to which the corresponding building unit may be derived from the hexagonal structure of $Bi_{6+\delta}S_{6+3\delta}Cl_{6-3\delta}$, in which all the bismuth atoms in the wall of the channel are crystallographically equivalent. These atoms, as well as Bi(1), in the intergrowth structure display very large values of eccentricity demonstrating the stereochemical activity of the lone pair of the bismuth atom.

Furthermore it can be deduced from Table 6 that (i) the coordination number of the constituting atoms in each substructure is maintained in the intergrowth structure and (ii) corresponding polyhedra with the same coordination number in the substructures as well as in the intergrowth structure display almost the same values of the polyhedron distortion parameters (*v*, *Ecc*$_v$, *Sph*$_v$).

Interestingly, the polyhedron around Bi(4), which acts as link between both building units in the intergrowth structure, presents almost the same values of the distortion parameters (*v*, *Ecc*$_v$, *Sph*$_v$) as the corresponding positions in the structures of $Bi_{6.88}S_{8.64}Cl_{3.36}$ and $Ag_{1.59}Bi_{3.42}S_{4.83}Cl_{2.17}$. This similarity is beneficial for the formation of a stress-free interface between the two structure modules.

In addition to the local similarity of the interfacial polyhedra in the three compounds, the formation of the intergrowth structure is also favored by two main factors:

(i) the metrical match of the (1 0 0) planes exhibited by the hexagonal structure of $Bi_{6.88}S_{8.64}Cl_{3.36}$ ($a \approx 11.54$ Å, $b \approx 4.04$ Å) and the monoclinic structure of $Ag_{1.59}Bi_{3.42}S_{4.83}Cl_{2.17}$ ($c \approx 11.80$ Å, $b \approx 4.04$ Å), and
(ii) the orientation of the connecting polyhedra around Bi(1) in the two substructures (Fig. 7).

The combination of these two structural units is so that the topology of the interfacial structure remains almost unchanged when they form the intergrowth structure. This structural analysis is consistent with the observation that single crystals of the three phases coexist in the same preparation.

Table 6
Comparison of the distortion of polyhedra around cations in (a) $Ag_{1.2}Bi_{17.6}S_{23}Cl_8$, (b) $Ag_{1.59}Bi_{3.42}S_{4.83}Cl_{2.17}$ and (c) $Bi_{6.88}S_{8.64}Cl_{3.36}$

Structure part	Atom	c.n.	Sphere radius (Å)	Sphere volume (Å^3)	Polyhedron volume (Å^3)	v	Ecc_v	Sph_v
Layer *A*	Bi(1)$^{(a)}$	7	2.99 ± 0.03	111	35.8	0.152	0.41	0.97
	Bi(1)$^{(b)}$	8	3.05 ± 0.13	119	49.5	0.014	0.49	0.87
Layer *B*	Bi(2)$^{(a)}$	6	2.79 ± 0.02	91	28.8	0.002	0.08	0.98
	Bi(2)$^{(b)}$	6	2.81 ± 0.05	93	29.5	0.006	0.05	0.94
Hexagonal tubes	Bi(1)$^{(c)}$	8	3.00 ± 0.07	113	46.5	0.015	0.38	0.93
	Bi(3)$^{(a)}$	8	3.03 ± 0.17	117	48.1	0.018	0.43	0.83
	Bi(4)$^{(a)}$	8	2.99 ± 0.07	112	46.6	0.007	0.43	0.93
	Bi(5)$^{(a)}$	8	3.02 ± 0.10	116	47.6	0.016	0.43	0.90
	Bi(6)$^{(a)}$	8	3.00 ± 0.04	113	46.7	0.009	0.40	0.96
	Bi(7)$^{(a)}$	8	3.00 ± 0.08	113	46.8	0.013	0.38	0.92
	Bi(8)$^{(a)}$	8	2.98 ± 0.07	111	45.9	0.013	0.43	0.93
Channel	Bi(9a)$^{(a)}$	9	3.20 ± 0.29	137	66.5	0.005	0.09	0.73
	Bi(2a)$^{(c)}$	9	3.16 ± 0.33	132	64.5	0.001	0.18	0.68
	Bi(9b)$^{(a)}$	6	2.95 ± 0.03	107	26.8	0.218	0.14	0.97
	Bi(2b)$^{(c)}$	6	2.90 ± 0.00	102	25.8	0.205	0.27	1.00
Layer *A*	Ag(1)$^{(a)}$	6	2.76 ± 0.13	88	27.2	0.030	0.00	0.86
	Ag(1)$^{(b)}$	6	2.77 ± 0.14	89	27.7	0.023	0.00	0.85
Connecting polyhedra	Bi(1)$^{(b)}$	8	3.05 ± 0.13	119	49.5	0.014	0.49	0.87
	Bi(1)$^{(c)}$	8	3.00 ± 0.07	113	46.5	0.015	0.38	0.93
	Bi(4)$^{(a)}$	8	2.99 ± 0.07	112	46.6	0.007	0.43	0.93

The calculation of sphere radius and standard deviation, sphere volume and polyhedron volume was performed with the program IVTON [26].

Acknowledgment

We thank Dr. Yurii Prots, Max Planck Institute for Chemical Physics of Solids in Dresden, for experimental support.

References

[1] E. Dönges, Z. Anorg. Allg. Chem. 263 (1950) 112–132.
[2] G.P. Voutsas, P.J. Rentzeperis, Z. Kristallogr. 152 (1980) 109–118.
[3] W. Haase-Wessel, Naturwissenschaften 60 (1973) 474.
[4] G.P. Voutsas, P.J. Rentzeperis, Z. Kristallogr. 166 (1984) 153–158.
[5] G.P. Voutsas, P.J. Rentzeperis, D. Siapkas, Z. Kristallogr. 177 (1986) 117–124.
[6] W. Haase-Wessel, Phase Transition 38 (1992) 127.
[7] K. Mariolacos, Acta Crystallogr. B 32 (1976) 1947–1949.
[8] G. Miehe, V. Kupčik, Naturwissenschaften 58 (1971) 219.
[9] V. Krämer, Acta Crystallogr. B 35 (1979) 139–140.
[10] J.C. Portheine, W. Nowacki, Z. Kristallogr. 141 (1975) 79–96.
[11] E. Makovicky, Z. Kristallogr. 173 (1985) 1–23.
[12] M. Ruck, Z. Anorg. Allg. Chem. 628 (2002) 453–457.
[13] M. Ruck, Z. Anorg. Allg. Chem. 628 (2002) 1537–1540.
[14] M. Ruck, P.F.P. Poudeu, T. Söhnel, Z. Anorg. Allg. Chem. 630 (2004) 63–67.
[15] P.F.P. Poudeu, M. Ruck, T. Söhnel, Z. Anorg. Allg. Chem. 630 (2004) 1276–1285.
[16] P.F.P. Poudeu, Ph.D. thesis, Technische Universität Dresden, Germany, 2004.
[17] E. Makovicky, W.G. Mumme, Can. Mineral. 17 (1979) 607–618.
[18] Analyse voyager, X-ray microanalysis and digital imaging, Noran Instruments System for Electron Microscope, Middleton, WI. USA.
[19] G.M. Sheldrick, SHELX-97, Program for Crystal Structure Determination, University Göttingen, Germany, 1997.
[20] N.E. Brese, M. O'Keeffe, Acta Crystallogr. B 47 (1991) 192–197.
[21] K. Brandenburg, DIAMOND, Visualization Tool System for Crystal Structures, Crystal Impact GbR, Bonn, 1999.
[22] B. Krebs, Z. Anorg. Allg. Chem. 396 (1973) 137–151.
[23] W.H. Zachariasen, Acta Crystallogr. 2 (1949) 288–291.
[24] T. Balić-Žunić, E. Makovicky, Acta Crystallogr. B 52 (1996) 78–81.
[25] E. Makovicky, T. Balić-Žunić, Acta Crystallogr. B 54 (1998) 766–773.
[26] T. Balić-Žunić, I. Vicković, IVTON, A Program for the Calculation of Geometrical Aspects of Crystal Structures and some Crystal Chemical applications, Geological Institute, University of Copenhagen.